Odontology
https://doi.org/10.1007/s10266-026-01562-6

ORIGINAL ARTICLE

Predicting the final color of layered resin composites from background-dependent optical measurements: a translucency-informed model

Mehmet Buldur[1] · **Bengü Doğu Kaya**[1] · **Berkant Sezer**[2]

Received: 3 June 2026 / Accepted: 24 August 2026
© The Author(s), under exclusive licence to The Society of The Nippon Dental University 2026

Abstract

The final color of layered resin composite restorations is influenced by complex optical interactions between composite layers and surrounding backgrounds. Therefore, this study investigated whether background-dependent optical measurements and translucency parameters could be used to predict final color coordinates and assessed model performance in an independent composite system. During model development, five composite shades (D3, D2, D1, E2, and E1) were used in both the 2-mm base and 1-mm top positions, generating all 25 possible ordered bilayer combinations. Background-dependent L*, a*, and b* coordinates and translucency parameters obtained from independent 1-mm and 2-mm layers were used to develop multivariable linear regression models for predicting the color coordinates of 3-mm layered specimens. Model performance was assessed using adjusted R^2, mean absolute error, root mean square error, and leave-one-out cross-validation. Independent-system evaluation was performed using 16 layered combinations from one additional composite system, and predictive accuracy was evaluated using CIEDE2000 color differences (ΔE_{00}). The regression models demonstrated adjusted R^2 values of 0.799, 0.843, and 0.964 for the L*, a*, and b* coordinates, respectively. During the independent-system evaluation, the mean ΔE_{00} value was 0.939 ± 0.333; 37.5% of the combinations were at or below the perceptibility threshold ($\Delta E_{00} \leq 0.8$), while all combinations (100%) were within the clinical acceptability threshold ($\Delta E_{00} \leq 1.8$). Background-dependent optical measurements and translucency parameters enabled accurate and clinically acceptable estimation of the final color coordinates of layered resin composites. The low prediction errors observed in one additional composite system provide preliminary evidence of predictive performance beyond the development material under standardized experimental conditions.

Keywords Translucency · Composite layering · Color prediction · Linear regression · Optical models

Introduction

Direct resin composite restorations have become an indispensable component of contemporary restorative dentistry because they combine minimally invasive treatment principles with favorable esthetic potential in both anterior and posterior teeth [1, 2]. However, achieving an imperceptible color match remains challenging because restorative success depends not only on reproducing tooth shade but also on harmonizing the optical interaction of the restoration with the surrounding dentition [3, 4]. Natural tooth color results from the optical interplay of enamel, dentin, pulp, and adjacent soft tissues, where light is scattered, absorbed, reflected, and transmitted through tissues with different thicknesses and translucencies [5]. Consequently, reproducing the natural appearance of dental tissues remains technique-sensitive and depends on the clinician's ability to emulate their layered optical architecture [3, 6].

In layered composite restorations, the final optical outcome is determined by interactions among restorative

✉ Mehmet Buldur
dtmehmetbuldur@gmail.com

[1] Faculty of Dentistry, Department of Restorative Dentistry, Çanakkale Onsekiz Mart University, Çanakkale, Türkiye, Turkey

[2] Faculty of Dentistry, Department of Pediatric Dentistry, Çanakkale Onsekiz Mart University, Çanakkale, Türkiye, Turkey

layers, their thicknesses, translucency/opacity levels, refractive behavior, and the optical characteristics of the underlying substrate [3, 7–9]. Natural teeth are multilayered structures in which enamel and dentin exhibit distinct optical properties, and contemporary layering approaches attempt to reproduce this arrangement using enamel- and dentin-like composite shades [3, 10, 11]. However, resin composites do not fully replicate the refractive and light-scattering behavior of natural dental tissues, making the final color of layered restorations difficult to predict [7, 9, 12]. Thinner and more translucent layers allow greater contribution from the underlying background, while changes in thickness can alter translucency and overall color perception [12–15]. Furthermore, resin composites may exhibit considerable differences in translucency and color response even when assigned the same nominal shade [16]. Thus, the optical behavior of layered composites is influenced by both background and thickness rather than being a fixed property of an individual shade [4, 7, 8]. Experimental studies have similarly shown that thickness, translucency, layering configuration, and material system can alter lightness, chroma, translucency, and overall color-matching behavior [17–20]. Clinically, these interacting variables make shade selection and layering highly experience-dependent, because the optical appearance of the individual composite layers does not necessarily predict the final appearance of the completed restoration. This difficulty in anticipating the cumulative color outcome provides a clinical rationale for investigating predictive approaches capable of estimating the final color of layered composites under standardized conditions.

Translucency is therefore a major determinant of composite esthetics because it governs both light transmission through the restorative layer and the contribution of the underlying substrate to the final color [5, 9, 10]. Accordingly, the same composite may exhibit different color coordinates over black, white, gray, or tooth-colored backgrounds, with greater background dependency as translucency increases or layer thickness decreases [13–15, 21]. These effects support the use of objective colorimetric measurements and translucency-related parameters rather than nominal shade designation alone for characterizing composite optical behavior [16, 17, 22]. Previous color-prediction approaches have included optical, spectral reconstruction, and regression-based methods. Kubelka–Munk-based approaches predict optical behavior from spectral reflectance data using material-specific absorption and scattering coefficients [19–21], whereas PCA-based methods reconstruct spectral reflectance from predefined sets of layered specimens [8]. More recently, thickness-dependent regression models have enabled direct estimation of CIE Lab* coordinates from color measurements obtained at different material thicknesses [23]. In contrast, the present approach uses the measured L*, a*, and b* coordinates of the individual component layers together with background-derived translucency parameters to directly estimate the final layered color. This avoids spectral reconstruction and the estimation of absorption and scattering coefficients while providing directly interpretable predictors. Moreover, the resulting equations were evaluated without recalibration in an independent composite system.

Despite advances in composite color prediction, reliable estimation of the final color of layered restorations remains challenging because translucency, layer thickness, substrate reflectance, scattering behavior, and stratification sequence interact to determine the final optical outcome [8, 11, 13, 15]. Moreover, available approaches frequently focus on descriptive optical analysis or rely on mathematically complex computational or reflectance-based models, which may limit their practical applicability [8, 19, 20, 24].

Many predictive models have also been evaluated under highly controlled conditions using specific materials or layer configurations, while evidence regarding their performance across independent restorative systems remains limited [8, 20, 23, 24]. Consequently, clinicians often continue to rely on empirical layering strategies and trial-and-error procedures to achieve esthetic integration [3, 9]. A simplified approach based on directly measurable optical characteristics of individual composite layers, particularly their background-dependent color behavior and translucency, may therefore provide a more practical framework for predicting the final color of layered restorations.

Therefore, the aim of the present study was to investigate whether the final color coordinates of layered resin composite restorations could be estimated using the optical measurements of individual composite layers obtained under different background conditions together with translucency-related parameters. In addition, the predictive performance of the proposed model was evaluated, without recalibration, in one composite system different from that used for model development. The null hypothesis tested was that optical measurements and translucency-related parameters of individual composite layers would not permit estimation of the final layered color within the predefined clinical acceptability threshold ($\Delta E_{00} \leq 1.8$).

Materials and methods

Study design

In this in vitro experimental study, it was investigated whether the final color of layered resin composite restorations could be predicted using a mathematical model developed from the background-dependent optical color

measurements and translucency-related optical parameters of the individual layers. The study consisted of two sequential phases: (1) development of the predictive model using an internal composite dataset and (2) evaluation of the model in one independent composite system. A schematic overview of the experimental workflow is presented in Fig. 1.

During the model development phase, five shades of Vittra APS Essential (FGM Dental Group, Joinville, SC, Brazil) were evaluated: D3, D2, and D1, designated by the manufacturer as dentin shades, and E2 and E1, designated as enamel shades. Each of the five shades was used in both the 2-mm base and 1-mm top positions, generating all 25 possible ordered combinations (5 × 5). Accordingly, the experimental set included dentin–dentin, dentin–enamel, enamel–dentin, and enamel–enamel combinations. This complete factorial arrangement was selected to provide the full set of ordered layer combinations required for model development and to capture a broader range of optical interactions between layers. Some combinations, including enamel-shade base layers beneath dentin-shade top layers, were included for experimental modeling purposes and were not intended to represent clinically recommended layering techniques.

To preliminarily assess predictive performance beyond the development material, an independent-system evaluation was performed using Tokuyama Estelite Sigma Quick resin composite shades (A1, A2, A3.5, and B2) selected according to the VITA classification, which differed from the composite system used during the model development process. Each of the four shades was used in both the 2-mm base and 1-mm top positions, generating all 16 possible ordered bilayer combinations (4 × 4). The independent evaluation system did not use the same dentin/enamel shade classification as the development material. The Estelite Sigma Quick system used for the independent-system evaluation consisted of body shades and did not include separate enamel- and dentin-shade categories. Although the selected shades represented differences in value, chroma, and hue, they may have provided a narrower range of translucency than the enamel and dentin shades used during model development. This difference was intentional because the predictive model was based on measured L*, a*, b*, and TP values rather than manufacturer-assigned dentin/enamel

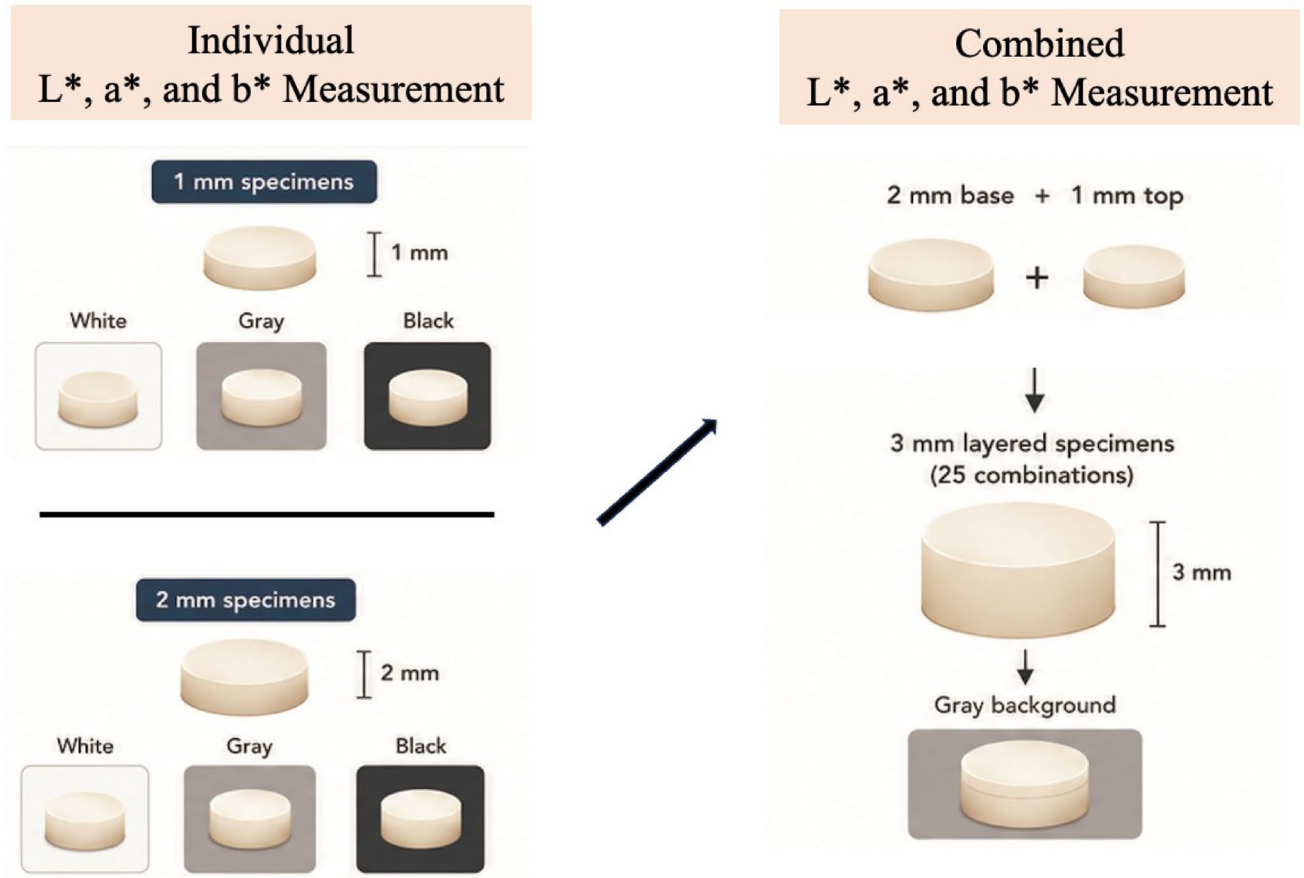


Fig. 1 Schematic representation of the experimental workflow. L*, a*, and b* coordinates of individual 1 mm and 2 mm composite specimens were measured over white, gray, and black backgrounds. The specimens were then combined to produce 3 mm layered composites, and their final color coordinates were measured over a gray background for regression model development and independent-system evaluation

shade categories, thereby allowing predictive performance to be evaluated across a different shade-designation system. Independent-system evaluation specimens were prepared using the same specimen geometry, layering configuration, and color measurement protocol. The composite shades selected for independent-system evaluation were chosen to represent differences in value, chroma, and hue within the available body-shade range. Detailed information regarding the composite materials used, manufacturer information, shades, and lot numbers is presented in Table 1. All model-development and independent-system evaluation combinations are presented in Supplementary Table S1.

Specimen preparation

Standard molds with a diameter of 8 mm and heights of 1 mm, 2 mm, and 3 mm, respectively, produced using 3D printers, were used for the preparation of the composite specimens. The layered specimens used during the model development phase were designed to have a total thickness of 3 mm, consisting of a 2 mm base layer and a 1 mm top layer. This standardized 2 mm + 1 mm configuration was selected to maintain a fixed layering geometry and to minimize the confounding effects of variable layer thickness or stratification sequence during model development and independent-system evaluation.

First, independent composite specimens with thicknesses of 2 mm and 1 mm were prepared. The composite materials were placed into the molds and polymerized only from their upper surfaces using an LED light-curing unit (Woodpecker i-LED, Guilin Woodpecker Medical Instrument Co., Guilin, China). The light-curing unit was used at a light output intensity of 1000–1200 mW/cm², and the tip of the device was positioned at a standardized minimum distance without contacting the specimen surface. A polymerization time of 20 s was applied for all specimens.

To obtain standardized, smooth, and reproducible specimen surfaces, a Mylar strip and glass slide were placed over the composite surface during the polymerization procedures. No additional finishing or polishing procedures were applied after polymerization in order to minimize additional surface-related variability during optical measurements. This approach was preferred to reduce surface irregularities and obtain more standardized spectrophotometric measurement conditions under controlled experimental settings. The thicknesses of all prepared specimens were verified at each stage using a digital caliper to ensure standardization.

Three independently prepared layered specimens were fabricated for each ordered bilayer combination. Accordingly, the model-development phase included 75 layered specimens (25 combinations × 3 specimens), whereas the independent-system evaluation phase included 48 layered specimens (16 combinations × 3 specimens). For each predefined ordered combination, the designated 1-mm top shade was applied over the corresponding polymerized 2-mm base shade. Subsequently, the specimens were polymerized only from their upper surfaces using the same light-curing unit and the same exposure duration (20 s), resulting in bilayer specimens with a total thickness of 3 mm. All specimens were prepared by the same operator.

Optical measurements and translucency analysis

All optical color measurements were performed using a VITA Easyshade 5 spectrophotometer (VITA Zahnfabrik, Bad Säckingen, Germany) operated in restorative measurement mode. The device was calibrated before each measurement session according to the manufacturer's instructions, and all measurements were recorded using the CIE Lab* color system. During the measurements, the spectrophotometer probe was positioned perpendicular to the specimen surface, and measurements were obtained from the center of each specimen. The device was completely repositioned between repeated measurements. All measurements were conducted under standardized ambient lighting conditions (5500 K) to minimize environmental light variability.

To evaluate the background-dependent optical behavior of the individual layers and layered specimens, optical measurements were performed using the black, white, and neutral-gray cards included in the same commercially available reference-card set (GC-2 Gy Card/White Balance Card Set, JJC, Shenzhen, China). The set was designed for

Table 1 Resin Composite Materials Used in the Study

Composites	Manufacturer	Composite Type	Monomers	Filler Content	Lot Number
Vittra APS Essential	FGM Dental Group, Joinville, SC, Brazil	Nanohybrid resin composite (Shades: D1, D2, D3, E1, E2)	UDMA, TEGDMA	Silanized radiopaque glass particles (40–60%), methacrylic monomers (15–25%), silicon dioxide (20–30%), APS photoinitiator composition (< 1%), stabilizers (< 1%) and pigments (< 1%)	130324
Estelite Sigma Quick	Tokuyama Dental, Tokyo, Japan	Supra-nano spherical resin composite (Shades: A1, A2, A3.5, B2)	Bis-GMA, TEGDMA	82 wt% (71 vol%) silica-zirconia and composite spherical submicron fillers (0.1–0.3 µm)	235M05

Vittra APS Essential dentin (D1, D2, D3) and enamel (E1, E2) shades were used during internal model development, whereas Estelite Sigma Quick shades (A1, A2, A3.5, and B2) were used for independent-system evaluation

photographic exposure and white-balance standardization and included a nominal 18% neutral-gray reference card together with white and black reference surfaces. The cards had flat, non-glossy surfaces, and the same physical cards were used throughout all measurement sessions. Before each measurement, the specimens were positioned in direct contact with the corresponding background surface using a consistent central measurement location and orientation. Black and white background measurements were used to quantify background-dependent color differences and calculate the translucency parameter, whereas the neutral-gray card was used as the predefined reference background for predictive modeling. Because manufacturer-certified CIE Lab* coordinates and spectral reflectance data were not available for these cards, they were treated as standardized experimental backgrounds rather than calibrated dental color standards. The neutral-gray background was selected as a predefined intermediate condition between the black and white backgrounds and was not intended to represent a universally optimal or more intrinsic reference background. Because separate prediction models based on black- or white-background measurements were not developed, the present study cannot determine whether use of the gray background improved model stability or predictive accuracy.

The independent 1-mm and 2-mm specimens were measured immediately after polymerization to characterize the optical properties of the individual component layers at the initial post-polymerization stage. The completed 3-mm layered specimens were measured after storage in distilled water at 37 °C for 24 h. The 24-h measurements were intended to represent the stabilized post-polymerization optical condition of the final layered specimens. For each independently prepared specimen/background combination, three consecutive spectrophotometric readings were obtained and averaged to generate a single specimen-level value. These repeated readings were considered technical measurements and were not treated as independent replicates. The specimen-level values obtained from the three independently prepared specimens within each ordered combination were subsequently averaged to generate a single combination-level value. Measurement position and device placement were standardized for all specimens, and all measurements were performed by the same researcher to minimize operator-related variation.

To evaluate the translucency properties of the composite specimens, the translucency parameter (TP) was calculated using the color coordinates obtained on black and white backgrounds according to the following formula:

$$TP = \sqrt{\left(L^*_W - L^*_B\right)^2 + \left(a^*_W - a^*_B\right)^2 + \left(b^*_W - b^*_B\right)^2}$$

The obtained TP values were incorporated into the predictive mathematical model as translucency-related variables representing the optical behavior of the individual layers.

Predictive modeling and independent-system evaluation

In this study, it was investigated whether the final L*, a*, and b* values of 3-mm-thick layered composite specimens on a gray background could be mathematically predicted using the optical measurements of the individual 1 mm and 2 mm layers constituting the same layered structure. During the predictive model development phase, the L*, a*, and b* values obtained on a gray background from the independently prepared 1 mm and 2 mm specimens, together with the translucency parameters (TP) calculated from the black and white background measurements, were used as independent variables. The dependent variables were the L*, a*, and b* values of the 3-mm layered specimens measured on a gray background after 24 h of water storage. Thus, the model was intentionally designed to evaluate whether optical measurements obtained from the individual component layers immediately after polymerization could predict the stabilized final color of the layered structure after 24 h. In the present study, separate multivariable linear regression models were constructed for the L*, a*, and b* coordinates to develop a simplified and interpretable predictive approach based on measurable optical parameters of individual composite layers. Although the optical behavior of layered resin composites involves complex phenomena, the primary aim of the model was to evaluate whether final color coordinates could be estimated at a clinically acceptable level under standardized conditions.

To assess predictive performance in one additional composite system, the regression equations obtained using the development dataset were directly applied to the independent-system evaluation dataset. During the independent-system evaluation phase, no recalibration or modification of the model coefficients was performed.

To evaluate model performance, the color differences between the L*, a*, and b* values predicted by the mathematical model and the actual spectrophotometrically measured L*, a*, and b* values in the independent-system evaluation dataset were calculated using the CIEDE2000 (ΔE_{00}) formula [25]. For interpretation of the ΔE_{00} values, the 50:50% perceptibility threshold (PT) and acceptability threshold (AT) were predefined as $\Delta E_{00} = 0.8$ and $\Delta E_{00} = 1.8$, respectively, based on established thresholds in dentistry [26]. These thresholds were defined a priori, before model-performance analyses were performed. In accordance with recommendations for dental color

assessment, the parametric weighting factors were set at 2:1:1 (kL: kC: kH) [27].

$$\Delta E_{00} = \sqrt{\left(\frac{\Delta L'}{K_L S_L}\right)^2 + \left(\frac{\Delta C'}{K_C S_C}\right)^2 + \left(\frac{\Delta H'}{K_H S_H}\right)^2 + R_T \frac{\Delta C'}{K_C S_C} \frac{\Delta H'}{K_H S_H}}$$

Additionally, ΔL*, ΔC*, and ΔH* values were also calculated to evaluate the effects of the error components on optical behavior.

Statistical analysis

Statistical analyses were performed using IBM SPSS Statistics Version 31.0 (IBM Corp., Armonk, NY, USA). Bootstrap and HC3 robust coefficient analyses were conducted using Python with the NumPy package. Continuous variables were expressed as mean±standard deviation. Separate multivariable linear regression models were constructed for each color coordinate to predict the final L*, a*, and b* values of the 3-mm-thick layered composite specimens on a gray background. In the regression analyses, the L*, a*, and b* values obtained on a gray background from the individual 1-mm and 2-mm-thick layers, together with the translucency parameters (TP) calculated from the black and white background measurements, were used as independent variables. The dependent variables were defined as the L*, a*, and b* values measured on a gray background for the 3-mm-thick layered specimens after 24 h of water storage. For predictive modeling, the analytical unit was the ordered bilayer combination. The values obtained from the three independently prepared specimens within each combination were averaged to provide a single combination-level observation. Accordingly, the regression analyses were based on 25 combination-level observations, whereas the independent-system evaluation was based on 16 combination-level observations. The 25 development observations represented the complete factorial set of all ordered combinations generated from the five selected shades rather than a sampled subset. The four predictors included in each coordinate-specific regression model were predefined according to the study hypothesis and were not selected through data-driven variable-selection procedures. Nevertheless, the resulting observation-to-predictor ratio was limited; therefore, the regression models were considered exploratory and their performance was interpreted cautiously.

Model performance was evaluated using the coefficient of determination (R^2), adjusted R^2, mean absolute error (MAE), and root mean square error (RMSE). Regression assumptions were assessed using variance inflation factor (VIF) values, residual normality assessment, homoscedasticity diagnostics, and influential observation diagnostics. Heteroscedasticity-consistent HC3 standard errors were used for coefficient-level inference. Unstandardized regression coefficients, HC3 robust standard errors, 95% confidence intervals, t statistics, and two-sided p-values were reported for each predictor. Given the exploratory nature of the predictive framework and the limited size of the development dataset, leave-one-out cross-validation (LOOCV) was performed to assess internal predictive stability and to determine the extent to which model performance was retained when individual combinations were omitted. LOOCV was not considered sufficient to eliminate the possibility of coefficient instability or optimistic performance estimates associated with the limited development sample. To further assess coefficient and model stability, nonparametric bootstrap resampling was performed using 5,000 resamples of the 25 combination-level observations. Bootstrap distributions, standard errors, and 95% percentile confidence intervals were obtained for the regression coefficients. Coefficient sign stability and optimism-corrected model-performance estimates were also evaluated. During the independent-system evaluation phase, the differences between the color coordinates predicted by the mathematical model and the actual spectrophotometrically measured values were calculated using the CIEDE2000 (ΔE_{00}) formula. Additionally, ΔL*, ΔC*, and ΔH* parameters were analyzed to evaluate the contribution of individual error components to the overall color difference.

Results

Regression model development

Separate multivariable linear regression models were constructed for each color coordinate to predict the final L*, a*, and b* values of the 3-mm-thick layered composite specimens on a gray background. The performance results of the regression models are presented in Table 2. The adjusted R^2 values were 0.799, 0.843, and 0.964 for the L*, a*, and b* models, respectively, with the highest value observed for the b* model. In addition, low MAE and RMSE values were obtained for all models. The regression coefficient estimates, HC3 robust standard errors, 95% confidence intervals, and coefficient-level significance tests are presented in Table 3. In all three models, the coordinate-specific measurements of both the 2-mm and 1-mm layers were independently associated with the corresponding final 3-mm color coordinate (all $p \leq 0.001$). The independent contribution of TP was less consistent across models. TP2mm was significantly associated with the final b* coordinate (B = −0.329, 95% CI: −0.607 to −0.052; $p = 0.022$), whereas the remaining TP coefficients did not reach statistical significance.

The final regression equations obtained using the internal model development dataset are presented below:

Table 2 Regression Model Development Performance

Model	Dependent Variable	*n*	R^2	Adjusted R^2	MAE	RMSE
Model 1	L*3 mm, grey	25	0.833	0.799	0.910	1.090
Model 2	a*3 mm, grey	25	0.869	0.843	0.318	0.408
Model 3	b*3 mm, grey	25	0.970	0.964	0.893	1.111

Higher R^2 and adjusted R^2 values together with lower MAE and RMSE values indicate better model fit and lower estimation error within the development dataset. All regression models were constructed using the optical measurements of the individual 1 mm and 2 mm composite layers together with their corresponding translucency parameter (TP) values

R^2 determination coefficient; *Adjusted R^2* adjusted determination coefficient, *MAE* mean absolute error, *RMSE* root mean square error

Table 3 Regression Coefficient Estimates for the Coordinate-Specific Prediction Models

Model	Predictor	B	HC3 SE	95% CI lower	95% CI upper	t	*p*
L* model	Intercept	-31.412	16.331	–65.479	2.654	-1.923	0.069
	L*2 mm, gray	0.704	0.119	0.456	0.953	5.914	<0.001
	L*1 mm, gray	0.631	0.160	0.297	0.965	3.939	0.001
	TP2mm	-0.220	0.194	–0.624	0.184	-1.138	0.269
	TP1mm	0.429	0.292	-0.179	1.037	1.472	0.156
a* model	Intercept	1.687	2.306	–3.124	6.498	0.732	0.473
	a*2 mm, gray	0.407	0.089	0.221	0.592	4.577	<0.001
	a*1 mm, gray	0.464	0.109	0.237	0.690	4.266	<0.001
	TP2mm	-0.138	0.069	–0.281	0.005	-2.015	0.058
	TP1mm	0.006	0.118	–0.240	0.252	0.050	0.961
b* model	Intercept	2.344	4.522	–7.089	11.777	0.518	0.610
	b*2 mm, gray	0.184	0.034	0.113	0.256	5.386	<0.001
	b*1 mm, gray	0.818	0.034	0.747	0.889	24.043	<0.001
	TP2mm	-0.329	0.133	–0.607	-0.052	-2.477	0.022
	TP1mm	0.182	0.252	–0.343	0.707	0.723	0.478

B, unstandardized regression coefficient; HC3 SE, heteroscedasticity-consistent HC3 standard error; CI, confidence interval; TP, translucency parameter. Coefficient-level inference was based on HC3 robust standard errors. The t statistics and p-values correspond to two-sided tests of the null hypothesis that the coefficient equals zero

Predictor notation: the coordinate-specific predictors represent the corresponding L*, a*, or b* values measured for the independent 2-mm and 1-mm layers on the gray background.

Table 4 Regression Diagnostics and Internal Validation Results

Model	Max VIF	Shapiro–Wilk *p*-value	Breusch–Pagan *p*-value	Adjusted R^2	LOOCV R^2	Optimism-corrected R^2	Layer-coordinate coefficient sign stability	Lowest TP coefficient sign stability
L* model	1.68	0.090	0.743	0.799	0.746	0.757	100.0%	87.8%
a* model	1.09	0.857	0.026	0.843	0.752	0.781	100.0%	47.8%
b* model	1.44	0.499	0.175	0.964	0.957	0.959	99.6–100.0%	79.8%

Lower VIF values indicate the absence of substantial multicollinearity. Shapiro–Wilk p-values > 0.05 suggest approximate residual normality, whereas Breusch–Pagan p-values > 0.05 indicate homoscedastic residual distribution. Optimism-corrected R^2 values were obtained from 5,000 nonparametric bootstrap resamples. Coefficient sign stability represents the percentage of bootstrap resamples in which the coefficient retained the same direction as in the original model. Layer-coordinate coefficient sign stability summarizes the 1-mm and 2-mm layer-specific color predictors; the lowest TP coefficient sign stability reports the less stable of the TP2mm and TP1mm coefficients within each model

VIF variance inflation factor, *LOOCV* leave-one-out cross-validation, *TP* translucency parameter

$$L*_{3mm,grey} = -31.412 + 0.704 \cdot L*_{2mm,grey} + 0.631 \cdot L*_{1mm,grey} - 0.220 \cdot TP_{2mm} + 0.429 \cdot TP_{1mm}$$
$$a*_{3mm,grey} = 1.687 + 0.407 \cdot a*_{2mm,grey} + 0.464 \cdot a*_{1mm,grey} - 0.138 \cdot TP_{2mm} + 0.006 \cdot TP_{1mm}$$
$$b*_{3mm,grey} = 2.344 + 0.184 \cdot b*_{2mm,grey} + 0.818 \cdot b*_{1mm,grey} - 0.329 \cdot TP_{2mm} + 0.182 \cdot TP_{1mm}$$

These regression equations were directly applied to the independent-system evaluation dataset without recalibration.

Regression diagnostics and model stability

The regression diagnostics and internal validation results are presented in Table 4. Low VIF values were obtained in all regression models. Residual analyses demonstrated that the residual distributions showed approximate normality across all models. Homoscedasticity assessments revealed homogeneous variance distributions in the L* and b* models, whereas mild heteroscedasticity was observed only in the a* model. Influential observation analyses did not identify any strong outlier substantially affecting the overall structure of the models. Leave-one-out cross-validation yielded R^2 values of 0.746, 0.752, and 0.957 for the L*, a*, and b* models, respectively. Bootstrap internal validation yielded optimism-corrected R^2 values of 0.757, 0.781, and 0.959, respectively. The coefficients of the 1-mm and 2-mm layer-specific color predictors showed high directional stability across bootstrap resamples, whereas greater variability was observed for some TP coefficients, particularly the TP1mm coefficient in the a* model.

Independent-system evaluation performance

To assess predictive performance in the additional composite system, the regression equations obtained from the internal dataset were directly applied to the independent-system evaluation dataset. The performance results of the independent-system evaluation are presented in Table 5. During the independent-system evaluation phase, the mean ΔE_{00} value was found to be 0.939 ± 0.333. The ΔE_{00} values ranged from 0.459 to 1.725. When the error components were examined, the lowest mean error was observed for the ΔH* parameter (0.441 ± 0.331), whereas relatively higher variation values were obtained for the ΔL* and ΔC* parameters. The distribution of the individual error components and the overall ΔE_{00} values across the layered composite combinations is presented in Fig. 2.

Table 5 Independent-System Evaluation Performance

Parameter	Mean Error	SD	Min	Max
ΔL*	0.794	1.052	-0.710	3.247
ΔC*	0.880	0.967	-1.330	2.094
ΔH*	0.441	0.331	0.075	1.282
ΔE_{00}	0.939	0.333	0.459	1.725

Lower values indicate smaller discrepancies between predicted and spectrophotometrically measured color coordinates in the independent-system evaluation dataset

SD standard deviation, *Min* minimum value, *Max* maximum value, *ΔL** lightness difference, *ΔC** chroma difference, *ΔH** hue difference, ΔE_{00} CIEDE2000 color difference

Measured and predicted color coordinates

The agreement between the measured and regression-predicted L*, a*, and b* coordinates for the independent-system evaluation dataset is presented in Fig. 3. The ΔE00 values ranged from 0.459 to 1.725, with the lowest value observed in the A2 + B2 combination and the highest value obtained in the A1 + A3.5 combination. Based on the predefined thresholds, 6 of 16 combinations (37.5%) showed ΔE00 values at or below the perceptibility threshold (≤0.8), whereas all 16 combinations (100%) were within the clinical acceptability threshold (≤1.8). However, relatively greater deviations were observed for the predicted b* coordinate in some independent-system evaluation combinations.

Discussion

The findings of the present study demonstrated that the combined evaluation of background-dependent optical measurements obtained from individual composite layers together with translucency-related parameters may be used to estimate the final color coordinates of layered resin composite restorations. In particular, the low ΔE_{00} values obtained in the independent-system evaluation dataset provide preliminary evidence of predictive performance beyond the development material under standardized experimental conditions. The present findings further support that the final optical behavior of layered restorations depends not only on nominal shade selection, but also on the translucency characteristics and background interactions of the individual composite layers. Accordingly, the null hypothesis was rejected under the present experimental conditions.

The overall predictive performance may be explained by the fact that the layer-specific L*, a*, and b* measurements provide empirical summaries of several material-dependent optical processes, including pigment absorption, filler- and resin-matrix-related light scattering, and refractive-index relationships. Previous studies have shown that composite materials assigned similar nominal shades may nevertheless exhibit different inherent color and translucency characteristics because of differences in their composition and optical coefficients [16]. Translucency also governs the extent to which the underlying substrate contributes to the apparent color of a restorative material, while background-dependent changes in L*, a*, and b* coordinates are closely related to TP [17, 22]. Therefore, the predictor set used in the present model may have captured both the coordinate-specific appearance of the individual layers and their susceptibility to background influence.

The coordinate-specific measurements of the individual layers were the most consistent independent predictors

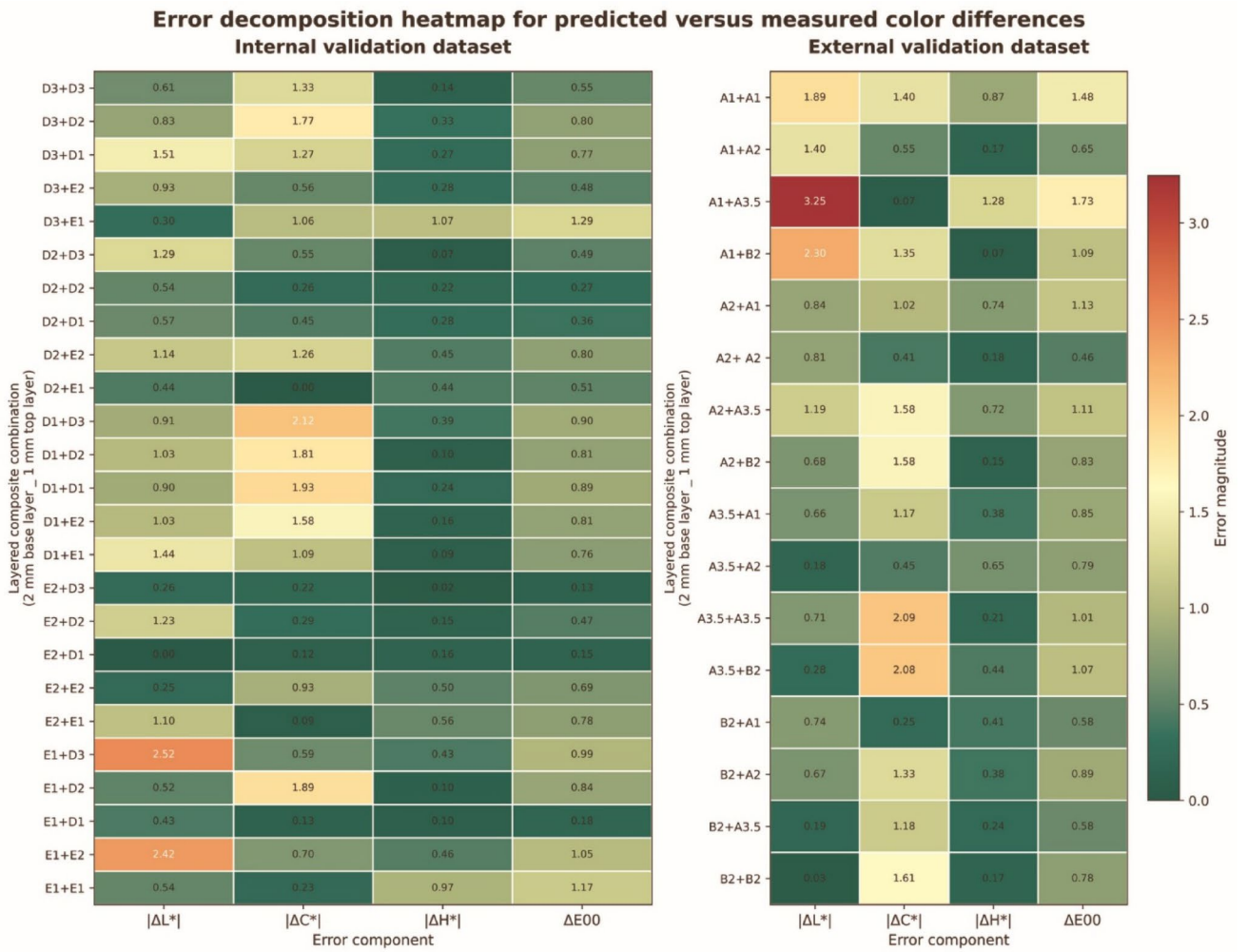


Fig. 2 Heatmap showing the distribution of |ΔL*|, |ΔC*|, |ΔH*|, and ΔE_{00} values for each layered composite combination in the development and independent-system evaluation datasets. Warmer colors indicate greater prediction error. In the layered composite combinations expressed as X + Y, X represents the 2 mm base layer and Y represents the 1 mm top layer

across the three models, whereas the additional contribution of TP varied according to the predicted color coordinate. This pattern should not be interpreted as indicating that translucency was unimportant. TP is derived from the color difference produced by black and white backgrounds, and previous studies have demonstrated significant relationships between translucency, lightness, chroma, and background-dependent changes in the CIE Lab* coordinates [17, 22]. Therefore, part of the translucency-related information may already have been represented within the gray-background L*, a*, and b* measurements, reducing the additional independent contribution of some TP terms. Nevertheless, the significant association of TP2mm with the final b* coordinate suggests that TP provided supplementary coordinate-specific information rather than a uniform contribution across all three models. However, because the present study did not directly compare the full models with reduced models excluding TP, the incremental contribution of TP to model fit and predictive accuracy cannot be determined.

The b* model showed the highest adjusted R^2 under the standardized conditions of the present study. Previous studies have reported associations between translucency, color coordinates, layer thickness, and refractive-index characteristics [12, 15, 16, 28]. However, the present study was not designed to determine why predictive performance differed among the individual color-coordinate models. Accordingly, the stronger internal performance of the b* model should be regarded as an empirical finding specific to the tested materials and protocol, particularly because adjusted R^2 reflects model fit within the development dataset rather than prediction accuracy in an independent material system. The relatively greater b* deviations observed in some independent-system evaluation combinations indicate that strong internal model fit did not ensure uniformly superior prediction in the independent composite system. This

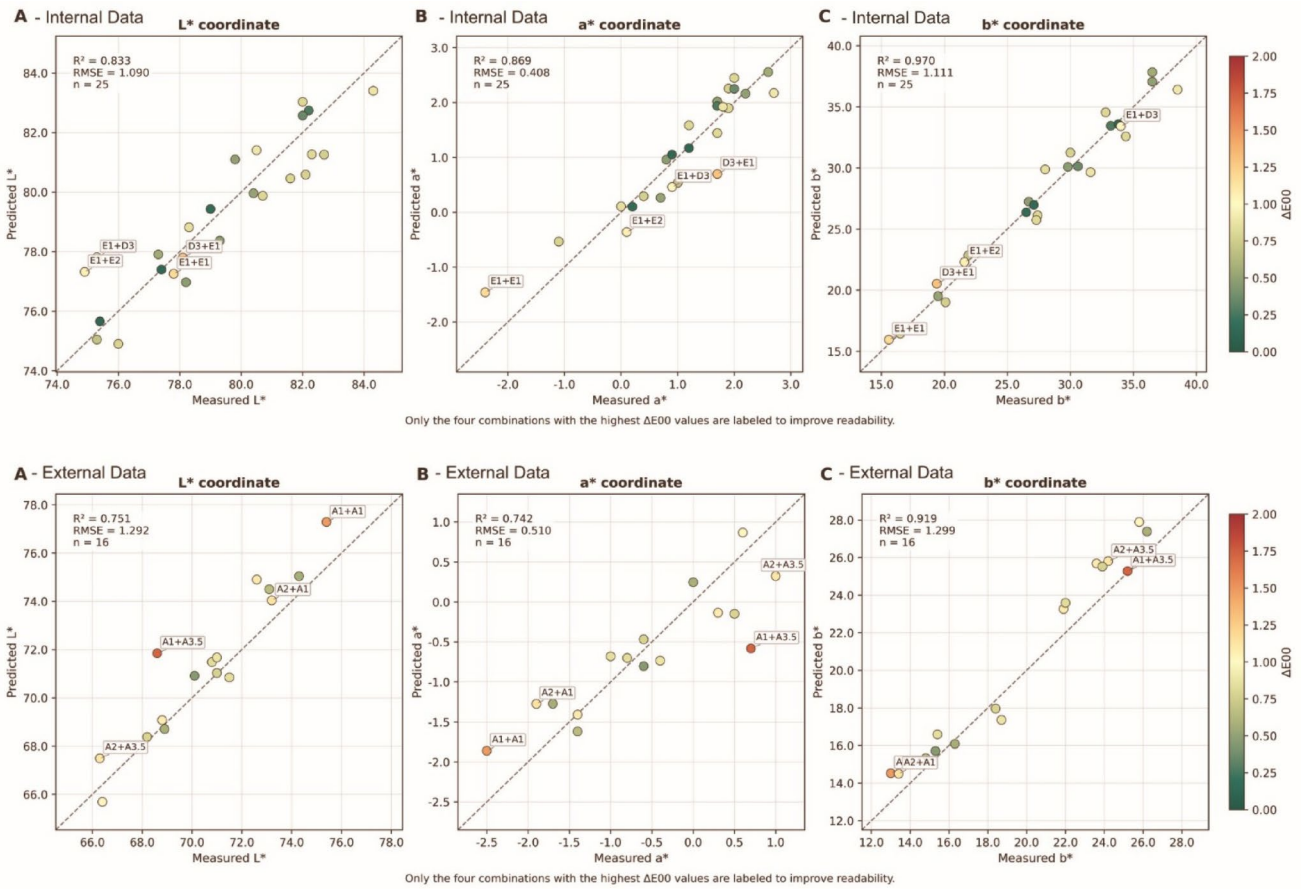


Fig. 3 Agreement between measured and regression-predicted L*, a*, and b* coordinates in the development and independent-system evaluation datasets. Dashed lines indicate perfect agreement (y = x). Point colors represent ΔE_{00} values, and only the four combinations with the highest ΔE_{00} values are labeled. In the layered composite combinations expressed as X + Y, X represents the 2 mm base layer and Y represents the 1 mm top layer

discrepancy may reflect combination-specific or material-specific optical behavior not fully represented by the development equations.

Prediction errors were not uniformly distributed across the independent-system evaluation combinations. The lowest ΔE_{00} value was observed for A2 + B2, whereas the highest value occurred for A1 + A3.5. The present design does not permit a definitive mechanistic explanation for these combination-specific differences. However, greater discrepancies may have arisen when the optical interaction between the base and top layers was not fully represented by the linear coordinate-specific equations or when the independent evaluation material exhibited composition-dependent scattering, absorption, pigment, or refractive-index behavior that differed from the development system. Previous studies have shown that composite materials with similar nominal shade designations may exhibit different inherent color and translucency characteristics and that the final appearance of layered restorations depends on the specific material combination and layering strategy [7, 16, 29]. Therefore, the observed error pattern may reflect material- and combination-specific optical interactions rather than a uniform loss of predictive performance.

Compared with physically based approaches such as Kubelka–Munk reflectance modeling, the present framework requires fewer intermediate optical measurements and produces directly interpretable coordinate-specific equations. Kubelka–Munk models can incorporate absorption and scattering coefficients, layer thickness, and backing reflectance and have been shown to predict the color of single- and double-layer composite structures within clinically acceptable limits [19, 20]. Thickness-dependent numerical and spectral approaches can estimate color across different material thicknesses [8, 23, 24]. Other predictive frameworks have reconstructed reflectance spectra from material-composition variables, such as the type and quantity of pigments, using nonlinear regression models [30]. However, these approaches generally require additional calibration specimens, spectral reflectance data, formulation-specific inputs, or more complex computational procedures.

In contrast, the present model uses directly measured L*, a*, b*, and TP values of the component layers and was applied to an independent composite system without coefficient recalibration. This relative simplicity is an advantage in terms of interpretability; however, it also limits the model's ability to directly represent wavelength-dependent absorption, scattering, and nonlinear optical interactions. Therefore, the present approach should be interpreted as a protocol-specific empirical prediction model rather than a general physical model of light transport.

The scope of the present model should consequently be defined narrowly. It can reasonably be expected to estimate the 24-h gray-background L*, a*, and b* coordinates of standardized bilayer specimens consisting of a 2-mm base layer and a 1-mm top layer when the optical properties of the individual layers are measured using the same spectrophotometric protocol. Its performance under different layering configurations, substrate or surrounding-color conditions, surface characteristics, and restorative materials requires further evaluation, as these factors are known to influence the optical behavior and color matching of resin composites [7, 13, 28, 31, 32].

Several limitations of the present study should be considered when interpreting the findings. The model-development dataset was limited to 25 combination-level observations, with four predefined predictors included in each coordinate-specific regression model. Although these observations represented the complete factorial set of all ordered combinations generated from the selected development shades, the limited observation-to-predictor ratio may have resulted in coefficient instability and optimistic internal performance estimates. LOOCV and bootstrap internal validation provided information regarding predictive consistency and coefficient stability but did not eliminate the limitations associated with the limited development dataset. These statistical diagnostics assess internal model consistency but cannot substitute for evaluation across a broader range of restorative materials. Therefore, the regression equations should be regarded as preliminary and require further evaluation in larger datasets including additional shades and composite systems. Because model development was based on a single composite system and independent-system evaluation on only one additional system, the robustness of the equations across materials with different compositions and optical characteristics remains uncertain. The independent-system evaluation was also limited to body shades of Estelite Sigma Quick, which may have represented a narrower translucency range than the enamel- and dentin-shade materials used for model development. Accordingly, future evaluations should include enamel-, body-, and dentin-shade composites covering broader, independently measured translucency ranges.

All data were obtained using standardized spectrophotometric measurements, and the complex clinical intraoral environment could not be fully simulated. Because only a standardized 2-mm base/1-mm top configuration was evaluated, the applicability of the model to other layer-thickness ratios or stratification sequences remains unknown [7, 11, 15]. The model was also evaluated under a single standardized illumination condition and hydration protocol; therefore, its performance under different illumination conditions and hydration states requires further investigation. Although the use of Mylar strips provided standardized and smooth specimen surfaces while reducing surface-related variability during spectrophotometric measurements, these surfaces may not fully represent the optical characteristics of clinically finished and polished composite restorations. In addition, the flat specimen geometry used in the present study does not reproduce the curved surfaces, variable restoration contours, internal reflections, surrounding tooth structures, and heterogeneous substrates encountered clinically.

Despite these limitations, translucency-informed predictive approaches may contribute to the development of future chairside digital layering simulations, AI-assisted shade-planning systems, or virtual restorative try-in applications [1]. However, the present findings should be regarded as proof-of-concept evidence under controlled laboratory conditions, and broader calibration, validation across multiple restorative systems, and incorporation of clinically relevant variables would be required before routine chairside use could be considered.

Conclusion

Within the limitations of the present study, translucency-informed predictive modeling based on background-dependent optical measurements of individual composite layers estimated the final color coordinates of layered resin composite restorations within the predefined clinical acceptability threshold under standardized laboratory conditions. The low color discrepancies observed in one additional composite system provide preliminary evidence of predictive performance beyond the development material; however, broader generalizability and direct clinical applicability remain to be established. Future studies should evaluate the performance of this approach across different material systems, layering configurations, surface treatments, and clinically relevant conditions.

Supplementary Information The online version contains supplementary material available at https://doi.org/10.1007/s10266-026-01562-6.

Acknowledgements The authors acknowledge the use of AI-assisted tools for language editing and grammatical refinement during manuscript preparation.

Author contributions MB: Conceptualization, Methodology, Investigation, Data Curation, Formal Analysis, Visualization, Writing – Original Draft. BDK: Methodology, Validation, Writing – Review & Editing. BS: Conceptualization, Supervision, Writing – Review & Editing.

Funding This research received no external funding.

Data availability The study data are available from the corresponding author upon reasonable request.

Declarations

Conflict of interest The authors declare no conflicts of interest.

Ethical approval This study was conducted entirely in-vitro and did not involve human participants, patient data, human tissues, or animals; therefore, ethical approval was not required.

References

1. Manauta J, Almeida G, Kovacs-Vajna ZM, et al. Precision layering techniques: Integrating digital tools for accurate color matching and realistic try-ins in anterior composite restorations. J Esthet Restor Dent. 2024;36(12):1638–50. https://doi.org/10.1111/jerd.13297.
2. Veloso SRM, Lemos CAA, de Moraes SLD, do Egito Vasconcelos BC, Pellizzer EP, de Melo Monteiro GQ. Clinical performance of bulk-fill and conventional resin composite restorations in posterior teeth: a systematic review and meta-analysis. Clin Oral Investig. 2019;23(1):221–33. https://doi.org/10.1007/s00784-018-2429-7.
3. Dietschi D, Fahl N Jr. Shading concepts and layering techniques to master direct anterior composite restorations: an update. Br Dent J. 2016;221(12):765–71. https://doi.org/10.1038/sj.bdj.2016.944.
4. Jouhar R, Ahmed MA, Khurshid Z. An overview of shade selection in clinical dentistry. Appl Sci. 2022;12(14):6841. https://doi.org/10.3390/app12146841.
5. Pecho OE, Ghinea R, do Amaral EA, Cardona JC, Della Bona A, Pérez MM. Relevant optical properties for direct restorative materials. Dent Mater. 2016;32(5):e105–12. https://doi.org/10.1016/j.dental.2016.02.008.
6. Fahl N Jr, Ritter AV. Composite veneers: The direct-indirect technique revisited. J Esthet Restor Dent. 2021;33(1):7–19. https://doi.org/10.1111/jerd.12696.
7. Ismail EH. Color interaction between resin composite layers: An overview. J Esthet Restor Dent. 2021;33(8):1105–17. https://doi.org/10.1111/jerd.12806.
8. Tejada-Casado M, Ghinea R, Pérez MM, et al. Color prediction of layered dental resin composites with varying thickness. Dent Mater. 2022;38(8):1261–70. https://doi.org/10.1016/j.dental.2022.06.004.
9. Villarroel M, Fahl N, De Sousa AM, De Oliveira OB Jr. Direct esthetic restorations based on translucency and opacity of composite resins. J Esthet Restor Dent. 2011;23(2):73–87. https://doi.org/10.1111/j.1708-8240.2010.00392.x.
10. Harnirattisai C, Kuphasuk W, Ruengrungsom C, Naorungroj S, Sattabanasuk V. Enamel layering using double-layered enamel-shade resin composites: The strategy to simulate the optical characteristics of human enamel. J Esthet Restor Dent. 2023;35(6):904–16. https://doi.org/10.1111/jerd.13072.
11. Betrisey E, Krejci I, Di Bella E, Ardu S. The influence of stratification on color and appearance of resin composites. Odontology. 2016;104(2):176–83. https://doi.org/10.1007/s10266-015-0197-2.
12. Oguro R, Nakajima M, Seki N, Sadr A, Tagami J, Sumi Y. The role of enamel thickness and refractive index on human tooth colour. J Dent. 2016;51:36–44. https://doi.org/10.1016/j.jdent.2016.05.010.
13. Perez BG, Gaidarji B, Palm BG, Ruiz-López J, Pérez MM, Durand LB. Masking ability of resin composites: Effect of the layering strategy and substrate color. J Esthet Restor Dent. 2022;34(8):1206–12. https://doi.org/10.1111/jerd.12942.
14. Santana MLC, Livi GJS, Santana TR, et al. Surrounding and background shades effect on color adjustment of single-shade composites. Braz Dent J. 2024;35:5742. https://doi.org/10.1590/0103-6440202405742. Published 2024 Jul 22.
15. Khashayar G, Dozic A, Kleverlaan CJ, Feilzer AJ, Roeters J. The influence of varying layer thicknesses on the color predictability of two different composite layering concepts. Dent Mater. 2014;30(5):493–8. https://doi.org/10.1016/j.dental.2014.02.002.
16. Mikhail SS, Schricker SR, Azer SS, Brantley WA, Johnston WM. Optical characteristics of contemporary dental composite resin materials. J Dent. 2013;41(9):771–8. https://doi.org/10.1016/j.jdent.2013.07.001.
17. Lee YK. Translucency of human teeth and dental restorative materials and its clinical relevance. J Biomed Opt. 2015;20(4):045002. https://doi.org/10.1117/1.JBO.20.4.045002.
18. Durand LB, Ruiz-López J, Perez BG, et al. Color, lightness, chroma, hue, and translucency adjustment potential of resin composites using CIEDE2000 color difference formula. J Esthet Restor Dent. 2021;33(6):836–43. https://doi.org/10.1111/jerd.12689.
19. Mikhail SS, Azer SS, Johnston WM. Accuracy of Kubelka–Munk reflectance theory for dental resin composite material. Dent Mater. 2012;28(7):729–35. https://doi.org/10.1016/j.dental.2012.03.006.
20. Mikhail SS, Johnston WM. Confirmation of theoretical colour predictions for layering dental composite materials. J Dent. 2014;42(4):419–24. https://doi.org/10.1016/j.jdent.2014.01.008.
21. Gouveia D, Yilmaz B, Cevik P, Johnston WM. Using Kubelka–Munk reflectance theory to predict optimal pink composite thickness and shade with an opaqued PEEK background for a final gingival color: An in vitro study. Dent Mater. 2022;38(9):1452–8. https://doi.org/10.1016/j.dental.2022.06.027.
22. Yu B, Lee YK. Influence of color parameters of resin composites on their translucency. Dent Mater. 2008;24(9):1236–42. https://doi.org/10.1016/j.dental.2008.01.016.
23. Tejada-Casado M, Ghinea R, Pérez MM, Ruiz-López J, Lübbe H, Herrera LJ. Development of thickness-dependent predictive methods for the estimation of the CIELab* color coordinates of monolithic and layered dental resin composites. Mater (Basel). 2023;16(2):761. https://doi.org/10.3390/ma16020761. Published 2023 Jan 12.
24. Tejada-Casado M, Duveiller V, Ghinea R, et al. Comparative analysis of optical and numerical models for reflectance and color prediction of monolithic dental resin composites with varying thicknesses. Dent Mater. 2024;40(10):1677–84. https://doi.org/10.1016/j.dental.2024.07.013.
25. Luo MR, Cui G, Rigg B. The development of the CIE 2000 colour-difference formula: CIEDE2000. Color Res Appl. 2001;26(5):340–50. https://doi.org/10.1002/col.1049.
26. Paravina RD, Ghinea R, Herrera LJ, et al. Color difference thresholds in dentistry. J Esthet Restor Dent. 2015;27(Suppl 1):S1–9. https://doi.org/10.1111/jerd.12149.

27. Perez Mdel M, Ghinea R, Herrera LJ, et al. Dental ceramics: A CIEDE2000 acceptability thresholds for lightness, chroma and hue differences. J Dent. 2011;39:e37–44. https://doi.org/10.1016/j.jdent.2011.09.007.
28. Ferraris F, Diamantopoulou S, Acunzo R, Alcidi R. Influence of enamel composite thickness on value, chroma and translucency of a high and a nonhigh refractive index resin composite. Int J Esthet Dent. 2014;9(3):382–401.
29. Varvara EB, Gasparik C, Ruiz-López J, Aghiorghiesei AI, Culic B, Dudea D. Color and translucency compatibility among various resin-based composites and layering strategies. Dent J (Basel). 2025;13(4):173. https://doi.org/10.3390/dj13040173. Published 2025 Apr 18.
30. Ghinea R, Pecho O, Herrera LJ, et al. Predictive algorithms for determination of reflectance data from quantity of pigments within experimental dental resin composites. Biomed Eng Online. 2015;14(Suppl 2):S4. https://doi.org/10.1186/1475-925X-14-S2-S4
31. Barros MS, Silva PFD, Santana MLC, Bragança RMF, Faria-E-Silva AL. Background and surrounding colors affect the color blending of a single-shade composite. Braz Oral Res. 2023;37:e035. . Published 2023 Apr 28. https://doi.org/10.1590/1807-3107bor-2023.vol37.0035. Published 2023 Apr 28. :e035.
32. Fernandes-E-Silva P, Furtado MD, Silva AFD, Piva E, Boscato N, Rosa WLOD. Influence of depth and translucency on the color matching of single-shade resin composites: An in vitro study. Braz Dent J. 2025;36:e246074. https://doi.org/10.1590/0103-6440202560 74. Published 2025 Apr 7.

Publisher's note Springer Nature remains neutral with regard to jurisdictional claims in published maps and institutional affiliations.

Springer Nature or its licensor (e.g. a society or other partner) holds exclusive rights to this article under a publishing agreement with the author(s) or other rightsholder(s); author self-archiving of the accepted manuscript version of this article is solely governed by the terms of such publishing agreement and applicable law.